创新团队成果专栏

# SHH激活型髓母细胞瘤中miRNA表达失调的分子机制

朱　颖，隋　怡，唐玉杰
上海交通大学基础医学院组织胚胎学与遗传发育学系，上海 200025

［摘要］**目的·**探究miRNA表达失调在SHH激活型髓母细胞瘤（sonic hedgehog-activated subtype medulloblastoma，SHH-MB）中的作用，并比较裸鼠皮下同种异体移植模型与实体瘤患者的失调miRNA的相关特征。**方法·**使用鼠源SHH-MB细胞系（SmoWT和SMB56）建立裸鼠皮下同种异体移植模型。每种模型被随机分为以平滑蛋白受体抑制剂（smoothened inhibitor，SMOi）GDC-0449灌胃处理的实验组、以二甲基亚砜（dimethyl sulfoxide，DMSO）灌胃的对照组，并收取这4组裸鼠的肿瘤样本。采集出生后7 d（P7）及60 d（P60）的正常裸鼠的小脑组织作为P7正常小脑、P60正常小脑组。参照肿瘤样本，收取GDC-0449灌胃处理的P7正常裸鼠的小脑组织（P7小脑给药组）以及DMSO灌胃处理的P7正常裸鼠的小脑组织（P7小脑对照组）。分别采用mRNA测序（mRNA sequencing，mRNA-seq）和miRNA测序（microRNA sequencing，miRNA-seq）获得以上8组样本的mRNA和miRNA表达数据并进行样本表达谱相关性分析。通过差异表达分析系统解析：① 鼠源SHH-MB模型的肿瘤核心转录组特征。② 正常小脑发育相关的转录组特征。③ 肿瘤及发育小脑中Hedgehog（Hh）通路依赖和非Hh通路依赖的转录组特征。利用miRDB、TargetScan与miRTarBase数据库并结合mRNA差异表达结果，预测关键差异miRNA的靶基因。通过京都基因与基因组百科全书（Kyoto Encyclopedia of Genes and Genomes，KEGG）富集分析，解析靶基因涉及的核心信号通路。针对在P7发育小脑中鉴定到的Hh通路依赖的miR-204-5p，进行靶基因预测与靶基因KEGG通路富集分析。最后，搜集R2与基因表达综合数据库（Gene Expression Omnibus，GEO）中SHH-MB患者肿瘤及健康对照小脑的mRNA与miRNA表达数据，通过差异表达分析与韦恩分析评估差异表达miRNAs/mRNAs调控关系在人与小鼠之间的保守性。**结果·**样本mRNA表达谱相关性分析显示，SmoWT对照组与SMB56对照组的mRNA表达谱相似性较高；2个对照组与P7正常小脑组的相似性高于P60正常小脑组，而GDC-0449处理未显著改变这2个对照组的整体转录组特征。miRNA表达谱相关性分析结果与mRNA层面类似。SmoWT对照组、SMB56对照组与P7正常小脑、P60正常小脑组的差异表达分析鉴定出2个对照组中共同显著上调的95个miRNA、下调的126个miRNA；其中50个上调miRNA和38个下调miRNA在P7与P60正常小脑比较中同向表达。通过SmoWT实验组与SmoWT对照组、SMB56实验组与SMB56对照组的差异表达分析，鉴定出各模型中Hh通路与非Hh通路依赖的miRNA。韦恩分析显示，Hh通路依赖的miRNA（占差异miRNA总数的10%~20%）在模型间重叠极少；非Hh通路依赖的miRNA则在模型间高度保守。Hh通路依赖的差异表达miRNA的靶基因的KEGG通路富集结果显示，其富集于磷脂酰肌醇3激酶/蛋白激酶B信号通路（phosphoinositide 3-kinase/protein kinase B pathway，PI3K/AKT）、磷脂酶D（phospholipase D，PLD）、RAS/丝裂原活化蛋白激酶信号通路（RAS/mitogen-activated protein kinase pathway，RAS/MAPK）和DNA复制（DNA replication）通路。通过比较P7小脑给药组与P7小脑对照组，鉴定出P7小脑中7个Hh通路激活和1个Hh通路抑制的miRNA，285个Hh通路激活和72个Hh通路抑制的mRNA。miR-204-5p的靶基因富集于细胞周期通路。SHH-MB患者肿瘤与健康小脑对照样本的差异表达分析鉴定出22个人鼠保守的miRNA，其靶基因富集于环磷腺苷（cyclic adenosine monophosphate，cAMP）和细胞周期通路等。**结论·**鼠源SHH-MB模型表现出广泛的miRNA表达失调，但SMOi处理仅对其中小部分失调miRNA有逆转作用，提示Hh通路对miRNA失调的影响有限，并且仅有非Hh通路依赖的失调miRNA在2个鼠源模型之间表现出部分重叠。此外，SHH-MB鼠源模型与实体瘤患者来源的肿瘤有保守的失调miRNA特征。

［关键词］SHH激活型髓母细胞瘤；Hedgehog通路；miRNA表达失调；小脑发育
［DOI］10.3969/j.issn.1674-8115.2026.01.001　［中图分类号］R739.41　［文献标志码］A

**[基金项目]** 国家自然科学基金（82473455，82293661）。
**[通信作者]** 唐玉杰，研究员，博士；电子信箱：yujietang@shsmu.edu.cn。
**[Funding Information]** National Natural Science Foundation of China (82473455, 82293661).
**[Corresponding Author]** Tang Yujie, E-mail: yujietang@shsmu.edu.cn.
**[网络首发]** https://link.cnki.net/urlid/31.2045.R.20260112.0840.002（2026-01-12 14:52:18）。

# Molecular mechanisms of miRNA expression dysregulation in SHH-activated subtype medulloblastoma

Zhu Ying, Sui Yi, Tang Yujie

*Department of Histoembryology and Genetic Development, Shanghai Jiao Tong University College of Basic Medical Sciences, Shanghai 200025, China*

**[Abstract]** **Objective**·To investigate the role of miRNA expression dysregulation in sonic hedgehog-activated subtype medulloblastoma (SHH-MB), and to compare the dysregulated miRNA features between subcutaneous xenograft models in nude mice and patients with solid tumors. **Methods**·Mouse SHH-MB cell lines (SmoWT and SMB56) were used to establish subcutaneous xenograft models in nude mice. For each model, mice were randomly divided into groups treated with the smoothened inhibitor (SMOi) GDC-0449 (SmoWT experimental group and SMB56 experimental group) or dimethyl sulfoxide (DMSO) (SmoWT control group and SMB56 control group), and tumor samples from these 4 groups were collected. Cerebellar tissues from normal P7 (postnatal day 7) and P60 nude mice were collected as controls (P7 normal cerebellum group and P60 normal cerebellum group). Following the same procedure, cerebellar tissues were also collected from P7 normal nude mice treated with GDC-0449 (P7 cerebellum treatment group) or DMSO (P7 cerebellum control group). mRNA sequencing (mRNA-seq) and microRNA sequencing (miRNA-seq) were performed on these eight sample groups to obtain mRNA and miRNA expression profiles. Subsequently, differential expression analysis was systematically employed to elucidate: ① the core transcriptomic features of tumors in mouse SHH-MB models; ② transcriptomic features associated with normal cerebellar development; ③ Hedgehog (Hh)-dependent and Hh-independent transcriptomic features in both tumors and developing cerebellum. Target genes of key differentially expressed miRNAs were predicted by integrating data from the miRDB, TargetScan, and miRTarBase databases, combined with mRNA differential expression results. Kyoto Encyclopedia of Genes and Genomes (KEGG) pathway enrichment analysis was then performed to identify core signaling pathways involving these target genes. Specifically, for the Hh-dependent miRNA miR-204-5p identified in the P7 developing cerebellum, target genes were predicted and subjected to KEGG pathway enrichment analysis. Finally, mRNA and miRNA expression profiles from SHH-MB patient tumors and healthy control cerebella were obtained from the R2 and Gene Expression Omnibus (GEO). Conservation of differentially expressed miRNAs/mRNAs and their regulatory relationships between humans and mice was then systematically assessed through differential expression and Venn analysis. **Results**·Analysis of mRNA expression profile correlations revealed a high correlation between the SmoWT control and SMB56 control groups. Both tumor control groups showed higher correlation with the P7 normal cerebellum group than with the P60 normal cerebellum group. Treatment with GDC-0449 did not significantly alter the overall transcriptomic profiles of either control group. The miRNA expression profile correlation results were consistent with those observed in the mRNA profiles. Differential expression analysis comparing the SmoWT control and SMB56 control groups with the P7 and P60 normal cerebellum groups identified 95 commonly upregulated and 126 commonly downregulated miRNAs in the two control groups. Among these, 50 upregulated and 38 downregulated miRNAs showed the same expression trends in the P7 and P60 normal cerebellum comparison. Differential expression analysis between the SmoWT experimental and control groups and between the SMB56 experimental and control groups identified Hh-dependent and Hh-independent differentially expressed miRNAs in each model. Venn diagram showed that the Hh-dependent miRNAs (accounting for 10%-20% of all differentially expressed miRNAs) showed minimal overlap between mouse SHH-MB models, whereas Hh-independent miRNAs were highly conserved across models. KEGG pathway enrichment analysis of the target genes of Hh-dependent differentially expressed miRNAs showed significant enrichment in the phosphoinositide 3-kinase/protein kinase B (PI3K/AKT) pathway, phospholipase D (PLD) pathway, RAS/mitogen-activated protein kinase (RAS/MAPK) pathway, and DNA replication pathways. Comparison between the P7 cerebellum treatment group and the P7 cerebellum control group identified 7 miRNAs and 285 mRNAs whose expression was promoted by the Hh pathway, and 1 miRNA and 72 mRNAs whose expression was inhibited by the Hh pathway in the P7 cerebellum. The target genes of miR-204-5p were enriched in the cell cycle pathway. Differential expression analysis of SHH-MB patient tumors *vs* healthy cerebellar controls identified 22 conserved human-mouse miRNAs, with their target genes enriched in the cyclic adenosine monophosphate (cAMP) signaling pathway and the cell cycle pathway. **Conclusion**·Mouse SHH-MB models exhibit extensive miRNA expression dysregulation. However, SMOi treatment reverses only a small subset of these dysregulated miRNAs, indicating a limited effect of the Hh pathway on miRNA dysregulation. Only Hh-independent dysregulated miRNAs show partial overlap between mouse SHH-MB models. Furthermore, there are conserved dysregulated miRNA features between mouse SHH-MB models and patients with solid tumors.

**[Key words]** sonic hedgehog-activated subtype medulloblastoma (SHH-MB); Hedgehog pathway; miRNA expression dysregulation; cerebellar development

髓母细胞瘤（medulloblastoma，MB）是最常见的儿童恶性脑肿瘤之一，约占所有儿童脑肿瘤的20%[1-2]。根据分子特征该细胞瘤主要被分为4种亚型，即WNT激活型（WNT-activated，WNT）、SHH激活型（sonic hedgehog-activated，SHH）、3型（Group 3，G3）和4型（Group 4，G4）[3-4]；其中，SHH激活型约占总病例的30%[5]。研究[6-8]显示SHH激活型髓母细胞瘤（sonic hedgehog-activated medulloblastoma，

SHH-MB）的关键分子特征是Hedgehog（Hh）通路的异常激活，常由*PTCH1*（patched 1）或*SUFU*（suppressor of fused）基因的失活性突变、平滑蛋白（smoothened，*SMO*）基因的激活性突变，以及*GLI2*（GLI family zinc finger 2）基因的扩增或转录激活等事件驱动。

Hh通路在小脑发育不同阶段的动态调控至关重要。以小鼠小脑为例：出生后第7日（P7）的小脑处于快速发育阶段，富集了大量Hh通路激活的颗粒神经元前体细胞（granule neuron precursor，GNP）；而在P60分化成熟的小脑中富集的是Hh通路沉默的颗粒神经元（granule neuron，GN）。同时，Hh通路也是SHH-MB的重要的治疗靶点。多种靶向Hh通路的正调控因子——SMO的抑制剂（smoothened inhibitor，SMOi）药物，如维莫德吉（vismodegib，研发代码GDC-0449）、索尼德吉（sonidegib，研发代码LDE225）和格拉德吉（glasdegib，研发代码PF-04449913）已获得美国FDA批准并进入针对SHH-MB的临床试验[9-10]。但其原发性和获得性耐药严重限制了SMOi药物的疗效；原发性耐药常由*SUFU*失活、*GLI2*或*MYCN*（N-myc）扩增等机制导致，获得性耐药常由*SMO*突变、*GLI2*扩增、旁通路激活［如RAS/丝裂原活化蛋白激酶（RAS/mitogen-activated protein kinase，RAS/MAPK）信号通路、磷脂酰肌醇3激酶/蛋白激酶B（phosphoinositide 3-kinase/protein kinase B，PI3K/AKT）信号通路等］导致[11-15]。因此，亟需探索新的分子机制和治疗靶点，以突破这一耐药瓶颈。

近年来，表观遗传学研究揭示了Hh通路在多层次上受到转录与转录后调控。DNA/RNA修饰、组蛋白修饰、染色质重塑及微小RNA（microRNA，miRNA）均可调节Hh通路活性，并影响肿瘤的发生与发展[16-17]。部分表观遗传抑制剂，如溴结构域和末端外翻抑制剂（bromodomain and extra-terminal inhibitor，BETi）、组蛋白去乙酰化酶抑制剂（histone deacetylase inhibitor，HDACi）、细胞周期依赖性激酶7抑制剂（cyclin-dependent kinase 7 inhibitor，CDK7i）和促核染色质转录因子抑制剂（facilitates chromatin transcription inhibitor，FACTi）等均已被证实能够阻断Hh通路并克服SMOi的耐药[18-21]。

miRNA是一类长度约22个核苷酸的非编码RNA，可通过与靶mRNA的3′非翻译区（3′ untranslated region，3′UTR）结合介导转录后调控，在肿瘤的发生发展中发挥双重作用[22-30]。已有研究报道，miR-125b、miR-324-5p和miR-326在SHH-MB中表达下调，并作为Hh通路的抑癌因子发挥作用[31-33]，miR-17/92基因簇在SHH-MB中显著高表达并发挥促癌作用[34-35]。然而，目前关于Hh通路依赖的miRNA表达调控在SHH-MB中的作用与机制尚缺乏系统阐释，且人源与鼠源模型之间的miRNA特征和功能差异尚未得到深入比较。基于此，本研究通过生物信息学分析，系统解析SHH-MB中的miRNA-mRNA调控网络，并探讨人源和鼠源的SHH-MB组织中miRNA-mRNA调控网络的保守性，为后续进行功能验证与靶向测试提供参考。

## 1　对象与方法

### 1.1　实验动物、细胞

BALB/c雌性裸鼠6～8周龄，购自上海灵畅生物科技有限公司，动物生产许可证为SCXK（沪）2023-0003，体质量为20~25 g。所有裸鼠饲养于上海交通大学医学院实验动物中心的标准笼中，使用许可证为SCXK（沪）2023-0041。于25 ℃、湿度50%~60%、12 h明暗交替、噪声<60 dB条件下进行饲养，裸鼠自由进食、饮水。

本研究使用了2个Hh通路自激活的鼠源SHH-MB细胞系（SmoWT和SMB56），SmoWT（基因型为*Trp53*$^{-/-}$ *Ptch*$^{+/-}$）受赠于斯隆-凯特林癌症研究所C. Rudin教授，SMB56（基因型为*Ptch*$^{+/-}$）受赠于丹娜-法伯癌症研究院Rosalind A. Segal教授。

### 1.2　主要试剂与仪器

高糖DMEM培养基（上海源培生物科技股份有限公司），Neurobasal-A培养基、DMEM/F-12培养基［含HEPES（4-羟乙基哌嗪乙磺酸）］、B27补充剂、青霉素-链霉素混合液、TrypLE™ Express酶（Gibco，美国），无血清细胞冻存液（苏州新赛美生物科技有限公司），TRIzol™试剂（Invitrogen，美国），脱氧核糖核酸酶Ⅰ（deoxyribonuclease Ⅰ，DNase Ⅰ）（Worthington，美国），Matrigel®基质胶（Corning，美国），生物安全柜、细胞培养箱（Thermo Fisher，美国）。

### 1.3　实验方法

1.3.1　细胞培养　于37 ℃、含5% $CO_2$的恒温培养箱中，采用Neurobasal-A培养基培养SmoWT细胞，

采用DMEM/F-12培养基（含HEPES）培养SMB56细胞，同时向上述培养基中添加2% B27补充剂和1%青霉素-链霉素混合液。该2种细胞均为悬浮培养，传代周期为7 d；第4日时按50%体积补充新鲜培养基继续培养，第7日时使用TrypLE™ Express酶进行消化，以将细胞团块解离为单细胞悬液用于传代，并在消化的同时加入DNase I以降低细胞黏附。待消化完成后，向其中加入磷酸盐缓冲液（phosphate buffered saline，PBS）以终止反应，所有消化步骤均在37 ℃恒温摇床上进行。

1.3.2 miRNA合成和功能相关基因的肿瘤依赖性分析 为探究miRNA合成与功能通路是否在肿瘤中发生全面失调，本研究对已发表的CRISPR-Cas9文库筛选数据[36]开展如下分析：首先，对SmoWT和SMB56细胞在体外培养、裸鼠皮下生长条件（即为筛选条件）下的筛选结果行韦恩分析，鉴定出在上述条件下均依赖的基因。接着，为量化miRNA合成和功能相关基因（*Drosha*、*Dgcr8*、*Ago2*、*Dicer1*和*Tarbp2*）的依赖性强弱，从上述文库筛选数据中提取其稳健秩聚合得分（robust rank aggregation score，RRA score），并进行排序、可视化处理。最后，为验证*Drosha*、*Dgcr8*的RRA score并非由个别sgRNA的脱靶效应导致，本研究进一步提取*Drosha*与*Dgcr8*的每条单链向导RNA（single-guide RNA，sgRNA）在筛选前后的测序读数，并进行可视化处理。

1.3.3 鼠源SHH-MB肿瘤和小脑组织样本的制备与测序 分别构建SmoWT和SMB56裸鼠皮下同种异体移植模型。具体步骤如下：将$1.5\times10^6$个SmoWT或SMB56细胞注射到裸鼠背部，待肿瘤体积达到1 000 $mm^3$时进行灌胃给药；将每种模型的裸鼠随机分为2组，一组接受1 000 mg/kg剂量GDC-0449（以下分别称为SmoWT实验组、SMB56实验组），另一组接受等浓度二甲基亚砜（dimethyl sulfoxide，DMSO）溶液作为对照（以下分别称为SmoWT对照组、SMB56对照组）；于上午、下午各给药1次，共计给药4次后终止实验，并采集该4组的移植肿瘤样本（以下简称“肿瘤样本”）。同时，为获得不同发育阶段的正常小脑转录本基线，收取未经任何处理的P7和P60正常裸鼠的小脑组织作为对照（记为P7正常小脑组、P60正常小脑组）。为探究Hh通路对正常发育小脑的作用，另取P7正常裸鼠，随机分为2组，分别以与前述实验相同方案的GDC-0449（P7小脑给药组）或DMSO（P7小脑对照组）进行灌胃处理，给药结束后收取小脑组织。

采用TRIzol™试剂裂解并保存上述8组样本，送至上海美吉生物公司分别进行RNA抽提及针对poly-A mRNA的建库、测序以获得mRNA-seq数据，以及进行RNA抽提及针对small RNA建库、测序以获得miRNA-seq数据。本实验中，每个处理条件均设置2个生物学重复（即2只裸鼠），且每只裸鼠的组织样本独立进行处理与分析。

1.3.4 mRNA-seq原始测序数据处理与转录组特征分析 利用TrimGalore工具对每个样本的原始测序数据进行接头类型检测和去除，而后使用STAR工具将序列比对至参考基因组GRCm38，再利用RSEM工具获得每个基因的表达量（counts、FPKMs和TPMs）。为评估生物学重复间的一致性以及不同组别样本间的表达谱相似性，使用R软件（v4.4.2）计算两两样本基因表达谱（TPMs）之间的Spearman相关系数。

基于基因的表达值（counts），使用DESeq2包进行多组差异表达分析，筛选阈值为adjust.$P$<0.05且$|\log_2FC|$>1。具体如下。

（1）肿瘤核心转录组特征：将SmoWT对照组与P7正常小脑组、P60正常小脑组分别进行差异表达分析；同样，将SMB56对照组与P7、P60正常小脑组分别行差异表达分析。对由此获得的差异表达mRNA进行韦恩分析，筛选出在2个SHH-MB模型中相较于P7或P60正常小脑均显著上调（或下调）的mRNA。

（2）小脑发育的转录组特征：将P7正常小脑组与P60正常小脑组进行差异表达分析，以鉴定在正常小脑发育过程中显著上调（或下调）的mRNA。

（3）肿瘤及正常发育小脑中的Hh通路及非Hh通路依赖的转录组特征：比较SmoWT实验组与SmoWT对照组，以及SMB56实验组与SMB56对照组得到显著差异表达mRNA即肿瘤中Hh通路依赖的mRNA，其余无显著差异的则为肿瘤中非Hh通路依赖的mRNA。同时，比较P7小脑给药组与P7小脑对照组得到显著差异表达mRNA即正常发育的小脑中Hh通路依赖的mRNA，其余为正常发育的小脑中非Hh通路依赖的mRNA。

1.3.5 miRNA-seq原始测序数据处理与转录组特征分析及差异表达miRNA的功能富集 使用Cutadapt工具对每个样本的原始测序数据进行接头去除，使用Bowtie工具将其比对至参考基因组GRCm38；随后基

于miRBase v22[37]数据库注释miRNA，并利用featureCounts进行定量以获得miRNA的表达矩阵（counts、CPMs）；最后，去除所有样本中CPMs总和小于1的低表达miRNA。样本间Spearman相关系数分析、差异表达分析均同“1.3.4”。

将得到的肿瘤核心转录组特征miRNA导入miEAA数据库（https://ccb-compute2.cs.uni-saarland.de/mieaa2/），限定研究物种为“Mus musculus”，进行疾病本体（Disease Ontology，DO）富集分析。

1.3.6　miRNAs/mRNAs调控对的鉴定　为系统阐释本研究中鉴定出的关键差异表达miRNA的潜在生物学功能，针对“1.3.5”筛选得到的显著差异表达miRNA，利用miRDB（http://www.mirdb.org/）、TargetScan（https://wwwtargetscanorg/）、miRTarBase（http://mirtarbase.mbc.nctu.edu.tw/php/index.php）数据库预测其潜在的下游靶基因；若某基因在任意数据库中被预测为特定miRNA的靶标，即被纳入候选靶基因，并将其与mRNA-seq差异表达结果进行整合。为筛选出高置信度的功能性调控关系，仅保留那些表达趋势相反的miRNAs/mRNAs对（即上调的miRNA对应下调的mRNA，或下调的miRNA对应上调的mRNA）。将最终获得的miRNAs/mRNAs调控对导入Cytoscape软件，利用“NetworkAnalyzer”工具进行可视化处理。

1.3.7　mRNA富集分析　使用R软件（v4.4.2）的clusterProfiler包对前述构建的miRNAs/mRNAs调控对中的mRNA所对应的基因（即靶基因）进行京都基因与基因组百科全书（Kyoto Encyclopedia of Genes and Genomes，KEGG）通路富集分析，筛选GeneRatio排名前十的信号通路。

1.3.8　人鼠保守miRNAs/mRNAs调控对的鉴定与分析　为鉴定在人类SHH-MB与鼠源模型中保守性miRNAs/mRNAs调控对，在R2数据库（https://hgserver1.amc.nl/cgi-bin/r2/main.cgi）中选择以下几个包含MB患者或健康对照小脑样本的mRNA数据集：① Pfister-223数据集（Tumor Medulloblastoma-Pfister-223-MAS5.0-u133p2），含223例不同亚型MB患者的表达数据。② Gilbertson数据集（Tumor Medulloblastoma-Gilbertson-76-MAS5.0-u133p2），含76例不同亚型MB患者的表达数据。③ Roth数据集（Normal Various-Roth-353-MAS5.0-u133p2和Normal Various-Roth-504-MAS5.0-u133p2），各含有9个健康对照小脑样本的表达数据。以上3个数据集均为U133 Plus 2.0阵列芯片检测得到，且其原始数据均采用MAS5.0算法进行标准化处理，因此将其合并（命名为“u133p2数据集”）后进行分析。

使用limma包对u133p2数据集中的SHH-MB患者样本与健康对照小脑样本的测序数据进行差异表达分析，筛选阈值为adjust.$P$<0.05且|$\log_2$FC|>1，得到差异表达mRNA。在基因表达综合数据库（Gene Expression Omnibus，GEO）（https://www.ncbi.nlm.nih.gov/geo/）中选择数据集GSE42657[38]，该数据集包含2例SHH-MB患者样本和3例正常成人小脑组织的miRNA芯片测序数据。使用limma包对SHH-MB患者样本与正常成人小脑组织进行差异表达分析，筛选阈值为adjust.$P$<0.1且|$\log_2$FC|>0.6，得到差异表达miRNA。为鉴定保守的调控关系，将上述获得的人类差异表达miRNA与“1.3.5”鉴定到的裸鼠皮下异种移植模型差异表达miRNA取交集，定义为“保守性差异表达miRNA”。采用与“1.3.6”相同的策略，筛选保守性差异表达miRNA的靶基因，得到“人鼠保守的miRNAs/mRNAs调控对”。对此调控对中的mRNAs，采用与“1.3.7”相同的方法进行KEGG通路富集分析。

### 1.4　统计学方法

采用GraphPad Prism 9.0软件和R软件（v4.4.2）进行统计分析和绘图。2组间比较采用非配对$t$检验，2组以上比较采用单因素方差分析。$P$<0.05表示差异具有统计学意义。

## 2　结果

### 2.1　miRNA合成与功能相关基因在鼠源SHH-MB中的依赖性分析

在以SmoWT和SMB56细胞为模型，分别于体外培养和裸鼠皮下生长条件下开展的靶向1 036个表观遗传相关基因的CRISPR-Cas9文库筛选中，*Drosha*和*Dgcr8*与先前报道[36]的*Cdk7*、*Cdk9*、*Cdk12*一样，均显示出高度保守的肿瘤依赖性（图1A）；在上述筛选条件下，*Drosha*和*Dgcr8*的依赖性排名均位于前20%（图1B），其表达缺失可显著抑制2个鼠源SHH-MB细胞在体外和体内条件下的生长和存活（图1C）。

A

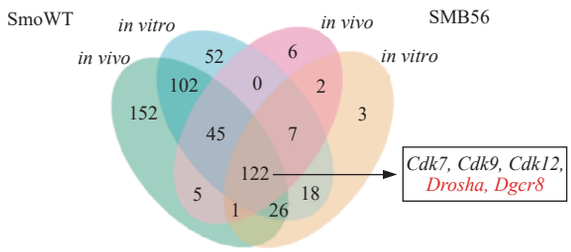


B

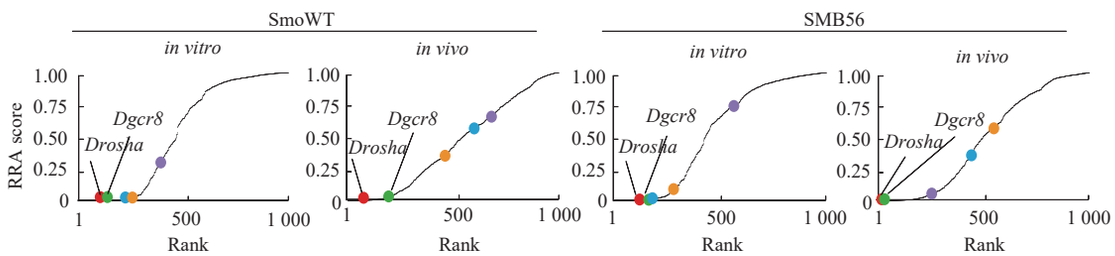


| | SmoWT *in vitro* | | | SmoWT *in vivo* | | | SMB56 *in vitro* | | | SMB56 *in vivo* | | |
|---|---|---|---|---|---|---|---|---|---|---|---|---|
| | *P* value | Rank | $Log_2FC$ | *P* value | Rank | $Log_2FC$ | *P* value | Rank | $Log_2FC$ | *P* value | Rank | $Log_2FC$ |
| ● *Drosha* | <0.001 | 102 | −2.514 | <0.001 | 78 | −3.922 | 0.006 | 121 | −1.167 | <0.001 | 12 | −3.476 |
| ● *Dgcr8* | <0.001 | 138 | −2.464 | <0.001 | 201 | −2.829 | 0.025 | 163 | −1.477 | <0.001 | 16 | −4.051 |
| ● *Ago2* | <0.001 | 227 | −1.206 | 0.147 | 621 | 0.325 | 0.027 | 164 | −1.033 | 0.583 | 457 | −0.155 |
| ● *Dicer1* | <0.001 | 262 | −1.091 | 0.036 | 478 | −0.450 | <0.001 | 262 | −1.091 | 0.776 | 567 | −0.031 |
| ● *Tarbp2* | <0.001 | 403 | −0.323 | 0.218 | 706 | −0.531 | 0.809 | 582 | 0.068 | 0.157 | 262 | −0.427 |

C

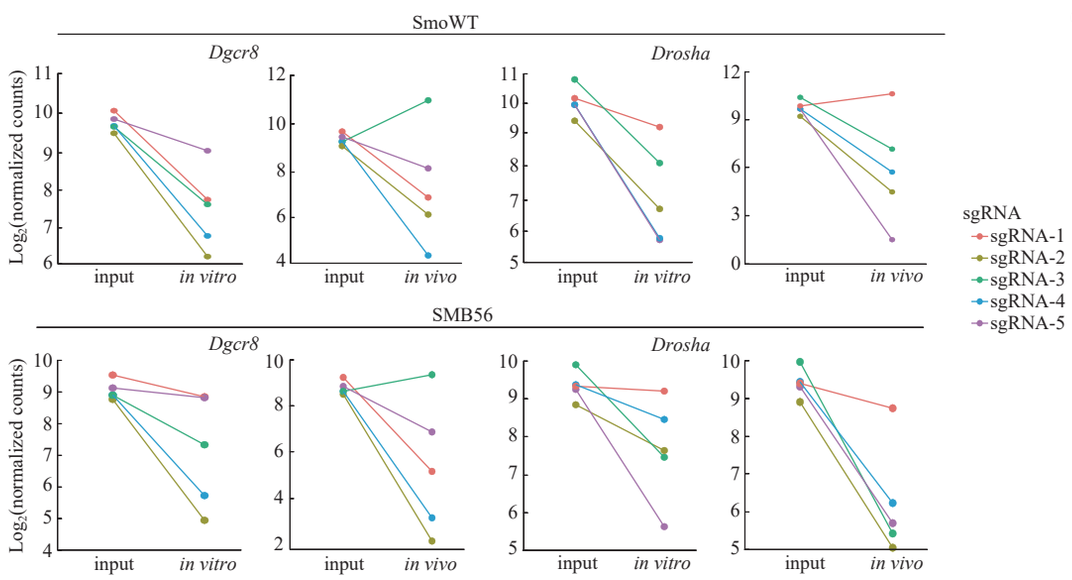


**Note**: A. Venn diagram of shared essential genes identified by CRISPR-Cas9 screening under *in vitro* and *in vivo* conditions in SmoWT and SMB56 cells. B. Detailed screening results for miRNA biogenesis genes *Drosha*, *Dgcr8*, *Ago2*, *Dicer1*, and *Tarbp2*. Genes were ranked by RRA score, which denotes gene essentiality, with lower scores representing stronger essentiality in the negative selection screen. C. Read count changes of sgRNAs targeting *Drosha* and *Dgcr8*.

**图1 miRNA合成与功能相关的基因在鼠源SHH-MB中的依赖性分析**

**Fig 1** Dependency analysis of miRNA biogenesis genes in mouse SHH-MB models

## 2.2 鼠源SHH-MB模型的mRNA转录组特征及miRNA合成与功能相关基因表达水平分析

对SmoWT实验组、SMB56实验组、SmoWT对照组、SMB56对照组、P7正常小脑组与P60正常小脑组的两两样本间mRNA表达谱进行相关性分析，结果（图2A）显示，SmoWT对照组与SMB56对照组的肿瘤样本之间转录组相似性较高；且该2个对照组与P7正常小脑组的相似性高于P60正常小脑组；GDC-0449处理并未显著改变2种SHH-MB模型的整体转录组特征。

将SmoWT对照组、SMB56对照组分别与P7正常小脑组、P60正常小脑组行差异表达mRNA的韦恩分析，结果显示：①共有1 192个基因显著上调，其中383个（约32.1%）在P7与P60正常小脑的比较中也显著上调

（图2B）。②共有2 579个基因显著下调，其中有1 015个（约39.4%）在发育过程中同样下调（图2C）。

分析图2A的6组样本中Hh通路关键转录因子Gli1和Gli2、miRNA合成和功能相关基因的mRNA表达水平，结果（图2D）显示Gli1和Gli2的mRNA表达变化完全符合预期：在P7正常小脑组中的表达显著

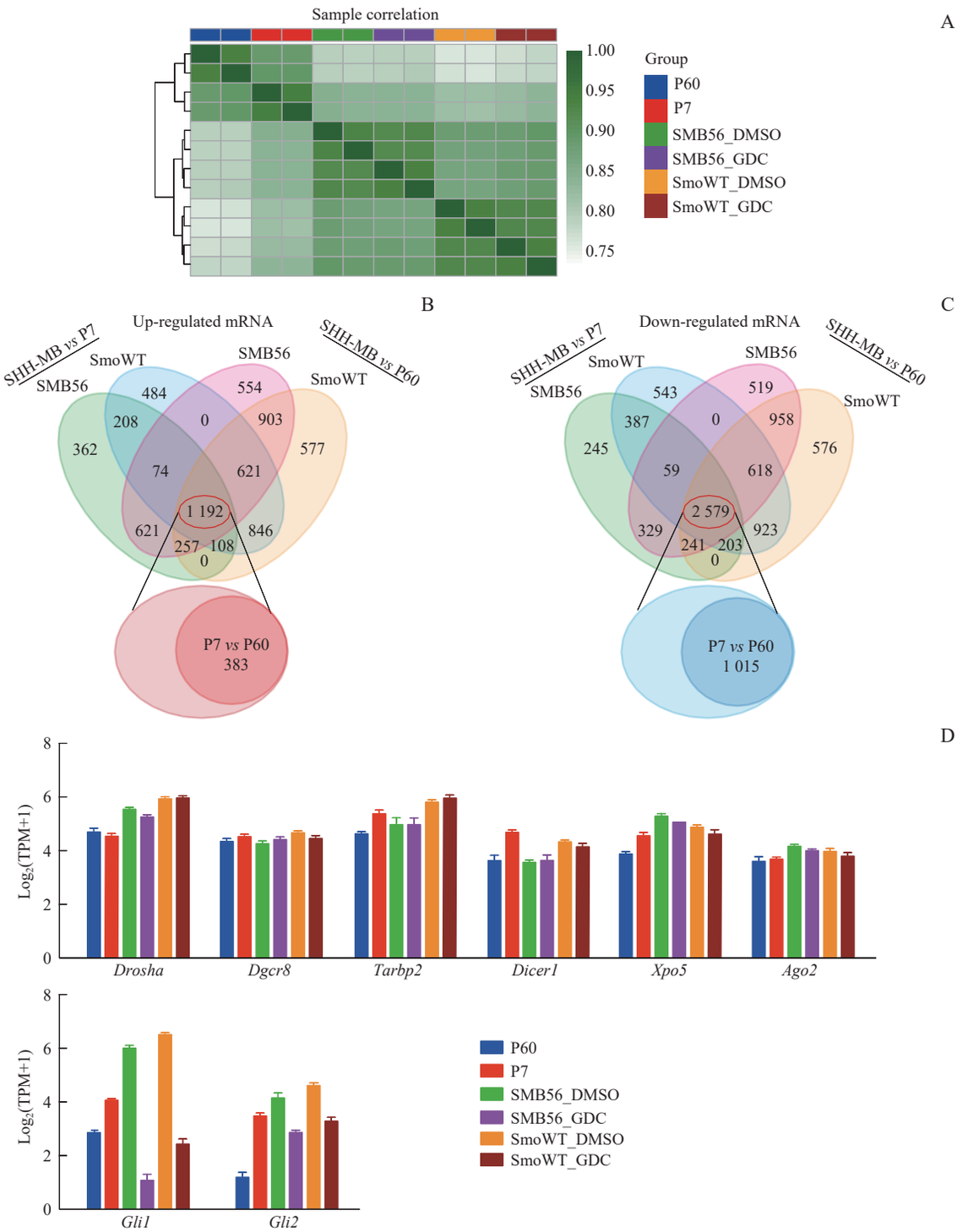


**Note**: A. Correlation analysis of mRNA expression profiles across sample groups, including SHH-MB tumors (SmoWT and SMB56 models with or without GDC-0449 treatment) and normal cerebellum (P7 and P60). B/C. Venn diagrams of the overlap of up-regulated mRNAs (B) and down-regulated mRNAs (C) among tumors *vs* P7 cerebellum, tumors *vs* P60 cerebellum, and P7 cerebellum *vs* P60 cerebellum. D. Expression levels of *Gli1*, *Gli2*, *Drosha*, *Dgcr8*, *Tarbp2*, *Dicer1*, *Xpo5*, and *Ago2* in the indicated groups.

**图2　鼠源SHH-MB模型与裸鼠正常小脑的mRNA转录组，以及Hh通路转录因子和miRNA生物合成相关基因的mRNA表达水平比较**

**Fig 2**　Comparison of mRNA transcriptomes between mouse SHH-MB models and normal nude mouse cerebellum, and mRNA expression levels of Hh pathway transcription factors and miRNA biogenesis genes

高于P60正常小脑组，在2种肿瘤对照组中表达最高，而GDC-0449处理可显著下调肿瘤中这2个mRNA的表达。miRNA合成与功能相关基因的mRNA水平在肿瘤组与正常小脑组之间，以及GDC-0449处理组与相应对照组之间均未发生显著变化。继而提示，该6组样本中miRNA的生物合成与加工过程整体上较为稳定，变化仅发生于部分特异性miRNA上。

### 2.3 鼠源SHH-MB模型的miRNA转录组特征及差异表达miRNA的DO富集分析

对SmoWT实验组、SMB56实验组、SmoWT对照组、SMB56对照组、P7正常小脑组与P60正常小脑组的两两样本间miRNA表达谱进行相关性分析，结果（图3A）显示，SmoWT对照组与SMB56对照组的肿瘤样本均与P7正常小脑组和P60正常小脑组

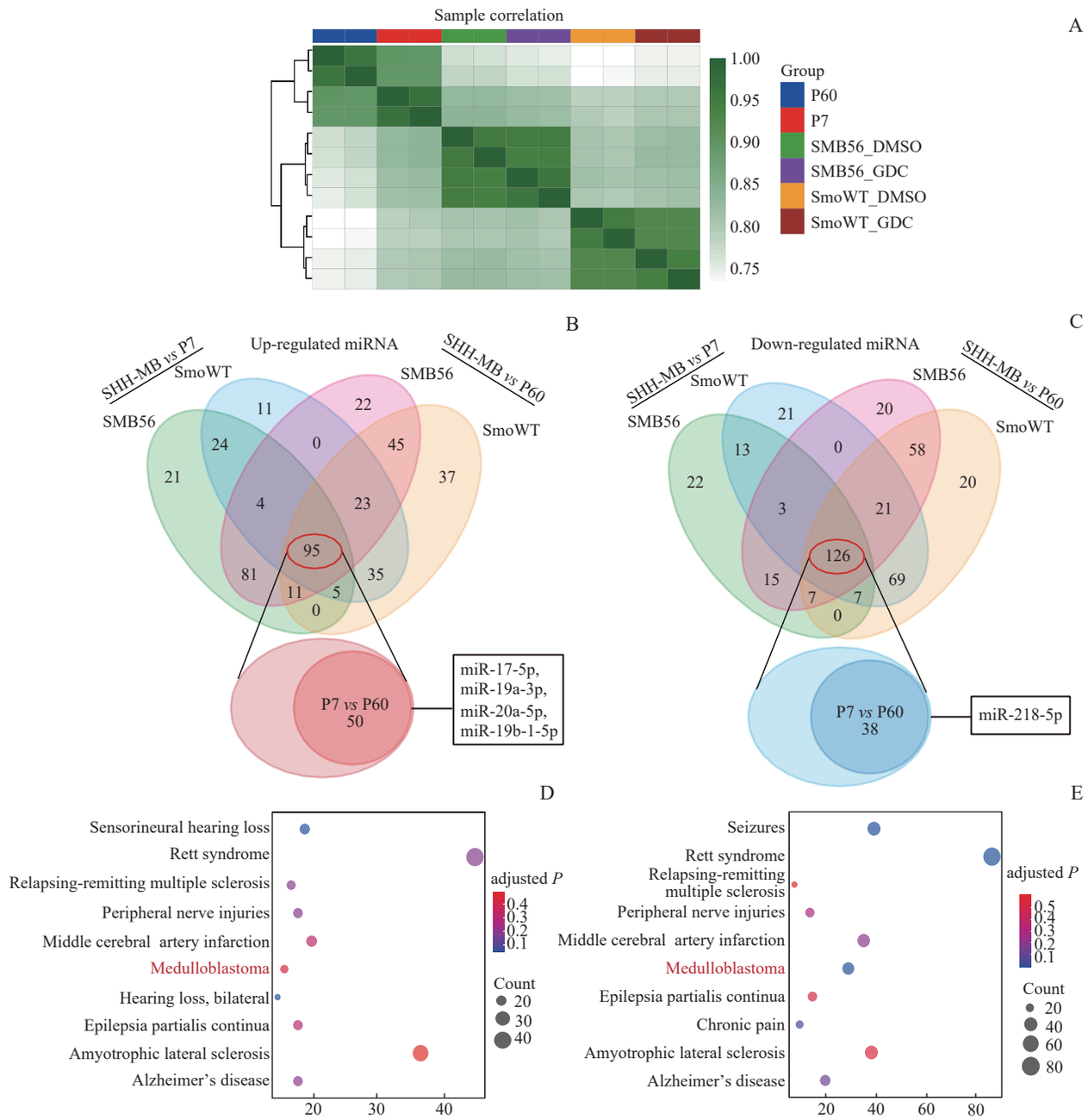


**Note**: A. Correlation analysis of miRNA expression profiles across sample groups, including SHH-MB tumors (SmoWT and SMB56 models with or without GDC-0449 treatment) and normal cerebellum (P7 and P60). B/C. Venn diagrams of the overlap of up-regulated miRNAs (B) and down-regulated miRNAs (C) among tumors *vs* P7 cerebellum, tumors *vs* P60 cerebellum, and P7 cerebellum *vs* P60 cerebellum. D/E. DO enrichment analysis of miRNAs consistently up-regulated (D) or down-regulated (E) in both mouse SHH-MB models.

**图3 鼠源SHH-MB模型与裸鼠正常小脑的miRNA转录组比较及差异表达miRNA的DO富集分析**

**Fig 3** Comparison of miRNA transcriptomes between mouse SHH-MB models and normal nude mouse cerebellum, and DO enrichment analysis of differentially expressed miRNAs

存在明显差异；GDC-0449处理未引起2个对照组样本miRNA表达谱的整体性改变；2个对照组样本与P7正常小脑组的相似性高于P60正常小脑组。

将SmoWT对照组、SMB56对照组分别与P7正常小脑组、P60正常小脑组行差异表达miRNA的韦恩分析，结果（图3B、C）显示：① 共显著上调95个miRNA，其中包含miR-17-5p、miR-19a-3p等多个miR-17/92家族成员；共显著下调126个miRNA，包括已知在SHH-MB中低表达的miR-218-5p。② 在这些共同失调的miRNA中，有50个共同上调的miRNA在P7与P60正常小脑的比较中也显著高表达；有38个共同下调的miRNA在P7与P60正常小脑的比较中也显著低表达。DO富集分析的结果显示，上述95个上调（图3D）、126下调（图3E）的miRNA与中枢神经系统疾病关联性最为显著，而MB是唯一富集到的肿瘤类型。

### 2.4　鼠源SHH-MB中Hh通路依赖与非Hh通路依赖的miRNAs/mRNAs分析

分析鼠源SHH-MB中Hh通路依赖的miRNA和mRNA。结果（图4A、B）显示：① 在2个SHH-MB模型中，Hh通路依赖的差异表达miRNA在全部差异表达miRNA中的占比较小（为10%~20%），mRNA层面呈现相似趋势，但比例高于miRNA层面。② 2个SHH-MB模型间，Hh通路依赖的失调miRNA重叠极少（上调4个、下调1个），非Hh通路依赖的miRNA则表现出高度保守性，而非Hh通路依赖的mRNA保守性更高。

对2个模型共有的Hh通路依赖miRNA的下游靶基因行KEGG通路富集分析，结果（图4C、D）显示，依赖Hh通路表达上调的miRNA，其靶基因富集于PI3K/AKT、磷脂酶D（phospholipase D，PLD）、RAS/MAPK信号通路；而受Hh通路抑制的miRNA，其靶基因则集中于细胞周期（cell cycle）与DNA复制（DNA replication）通路。

### 2.5　正常发育小脑中Hh通路依赖与非Hh通路依赖的miRNAs/mRNAs分析

对P7小脑给药组、P7小脑对照组与P60正常小脑组的miRNA表达谱和mRNA表达谱的相关性分析进行分析，结果（图5A）显示GDC-0449处理虽未显著改变P7正常小脑的miRNA表达谱，但使其mRNA表达谱向P60正常小脑的状态趋近。对正常发育小脑中Hh通路依赖的miRNA和mRNA进行分析，结果（图5B、C）显示P7小脑中依赖Hh通路负向调控的miRNA和mRNA分别为1个和72个，依赖Hh通路正向调控的miRNA和mRNA分别为7个和285个，包括已知的Hh通路相关基因（*Gli2*、*Ptch2*、*Cdk6*）、在肿瘤中作为Hh通路抑制因子发挥作用的*Usp44*[25]、小脑发育和SHH-MB形成的主调控因子*Atoh1*[26]以及细胞周期调控因子*E2f2*[39]等。对图5B中显示的P7小脑依赖Hh通路下调的miR-204-5p进行下游靶基因预测，结果（图5D、E）显示靶基因（如*Aurkb*、*Ccnd1*、*Ccnd2*）显著富集于细胞周期通路。

### 2.6　SHH-MB患者肿瘤组织中的miRNAs/mRNAs表达特征及其与人鼠保守性分析

对SHH-MB患者样本与健康对照小脑样本的mRNA测序数据进行表达水平分析，结果（图6A）显示，SHH-MB患者样本中GLI1与GLI2的mRNA水平显著高于健康小脑对照，而核心miRNA合成基因的表达则未呈现一致性的失调趋势。对miRNA测序数据分析后发现，2例SHH-MB肿瘤样本间存在较高的异质性（图6B），共鉴定出17个上调和16个下调的差异表达miRNA（图6C）。值得注意的是，其中约2/3的miRNA（22/33）至少在1种鼠源SHH-MB模型中呈现同向的表达失调，显示出较高的人鼠保守性（图6D）。这些保守miRNA包含了已报道的在SHH-MB中有重要促癌作用的miR17-92簇（miR-18a-5p和miR-106b-5p）和在肿瘤中有拮抗Hh通路作用的miR-330-5p和miR-338-3p[40-41]。

为寻找人鼠保守的miRNAs/mRNAs调控对，本研究首先对差异表达miRNA与mRNA的跨物种保守性进行分析。韦恩图的结果（图6E）显示，在2个鼠源模型共同上调的2 973个mRNA中，有922个（约占31.0%）在人类SHH-MB中也上调；在2个鼠源模型共同下调的4 396个mRNA中，有1 460个在人类SHH-MB中也下调。基于这些保守的miRNA与mRNA，构建保守的miRNAs/mRNAs调控对并对其中的mRNA进行KEGG功能富集分析，结果发现保守的上调miRNA的靶基因主要参与环磷腺苷（cyclic adenosine monophosphate，cAMP）信号通路、胞吞作用以及众多神经相关分子过程（图6F），其中cAMP信号通路的激活已被证实能够显著拮抗Hh通路[42]；保守的下调miRNA的靶基因主要参与细胞周

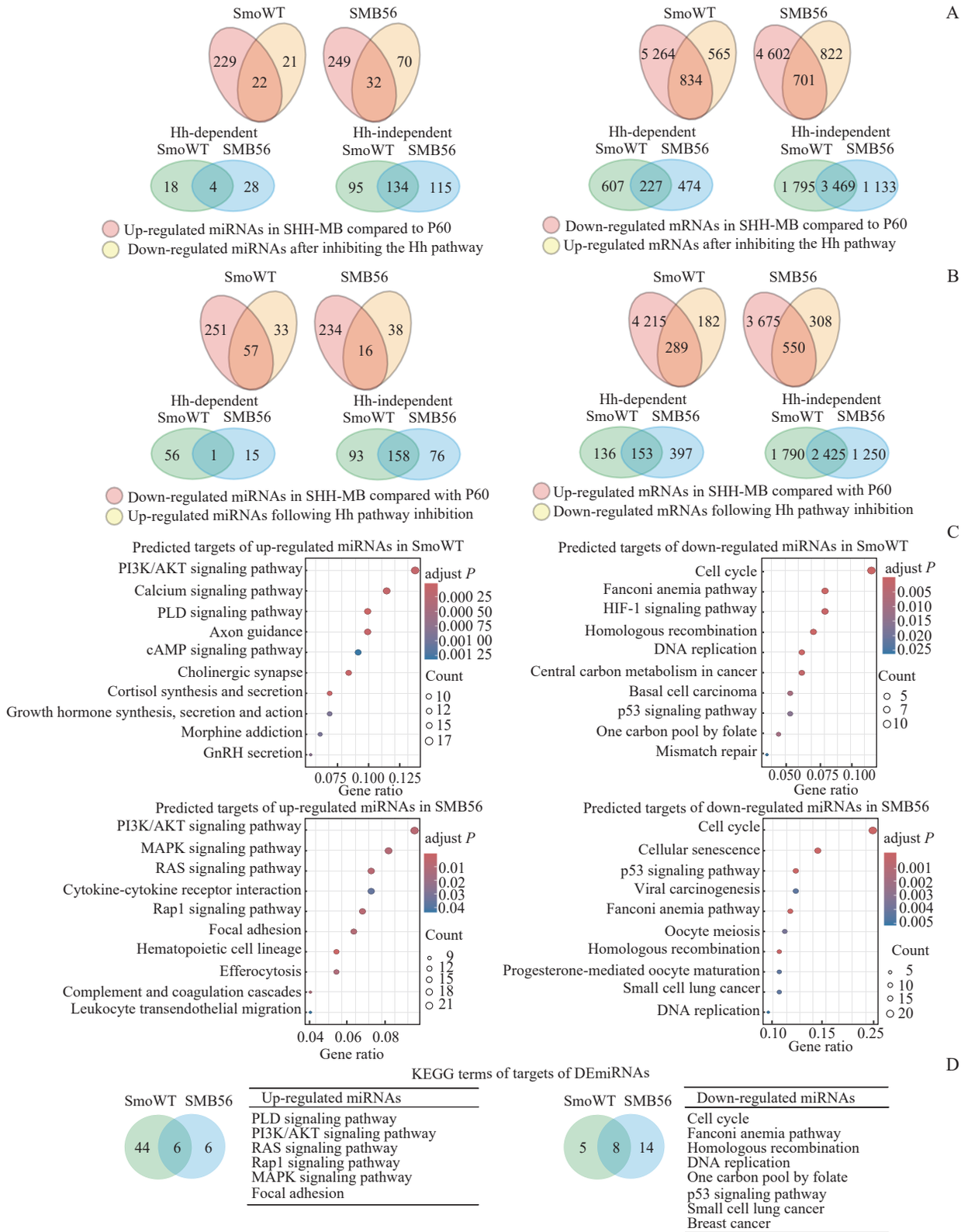


**Note**：A/B. Identification and overlap of Hh-dependent and Hh-independent tumor-upregulated miRNAs and tumor-downregulated mRNAs (A), and tumor-downregulated miRNAs and tumor-upregulated mRNAs (B). C. KEGG enrichment analysis of predicted target genes of Hh pathway-dependent miRNAs/mRNAs. D. Venn diagrams of the overlap of KEGG terms between mouse SHH-MB models in Fig C. cAMP—cyclic adenosine monophosphate; GnRH—gonadotropin-releasing hormone; HIF-1—hypoxia-inducible factor-1; RAS—rat sarcoma viral oncogene; Rap1—ras-related protein 1; DEmiRNAs—differentially expressed miRNAs.

**图4　鼠源SHH-MB模型中差异表达miRNAs/mRNAs的Hh通路依赖性及KEGG通路富集分析**

**Fig 4**　Hh pathway dependence of differentially expressed miRNAs/mRNAs and KEGG pathway enrichment in mouse SHH-MB models

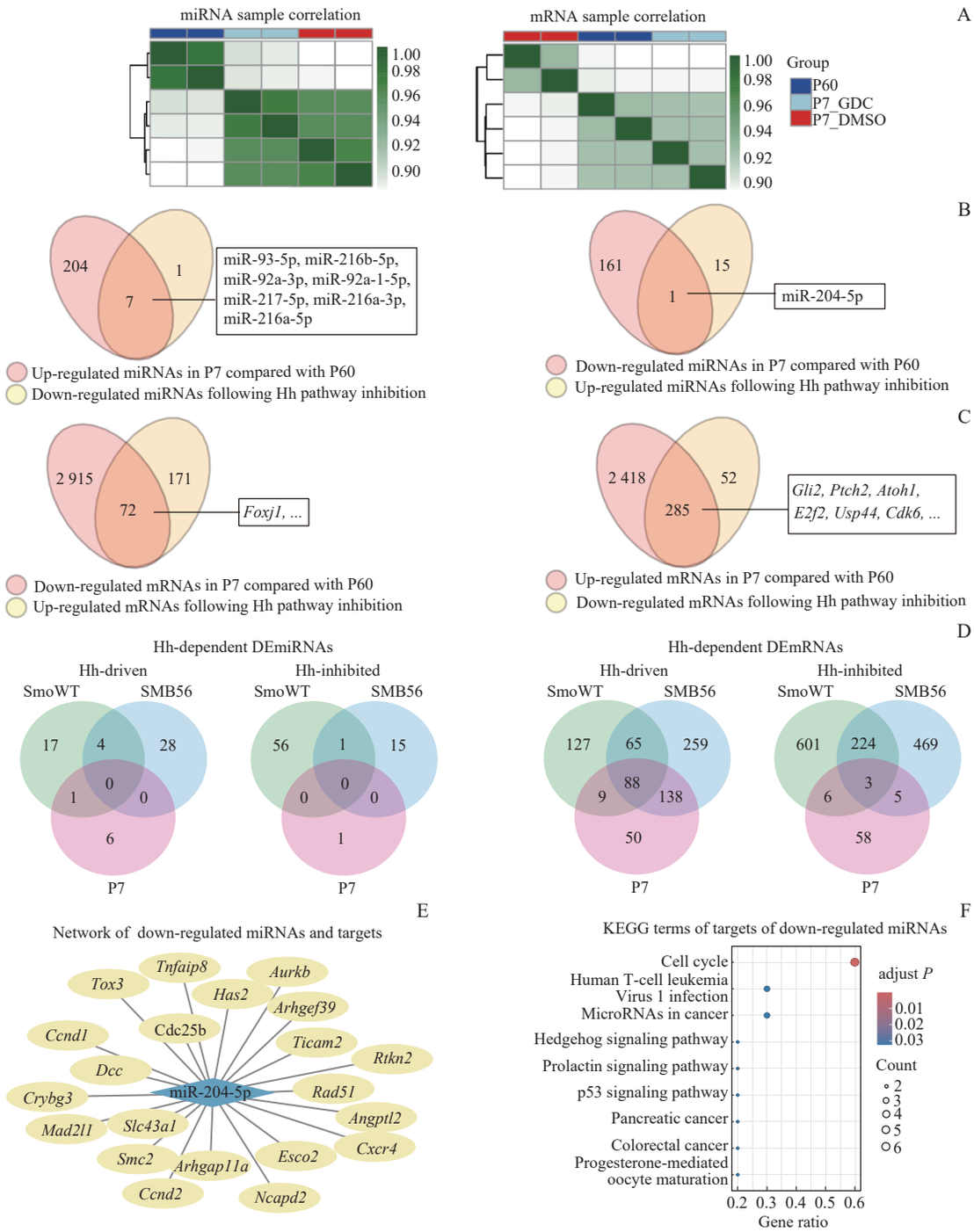


**Note**：A. Correlation analysis of miRNA and mRNA expression profiles across P60 cerebellum and DMSO-treated or GDC-0449-treated P7 cerebellum. B. Identification of Hh pathway-dependent differentially expressed miRNAs in the P7 cerebellum. C. Identification of Hh pathway-dependent differentially expressed mRNAs in the P7 cerebellum. Foxj1—forkhead box J1; Gli2—GLI family zinc finger 2; Ptch2—patched 2; Atoh1—atonal homolog 1; E2f2—E2F transcription factor 2; Usp44—ubiquitin specific peptidase 44; Cdk6—cyclin-dependent kinase 6. D. Venn diagrams of the overlap of Hh pathway-dependent miRNAs and mRNAs among mouse SHH-MB models and the P7 cerebellum. E. Regulatory network of miR-204-5p and its predicted target genes. *Tox3*—TOX high mobility group box family member 3; *Tnfaip8*—TNF alpha-induced protein 8; *Aurkb*—aurora kinase B; *Has2*—hyaluronan synthase 2; *Arhgef39*—Rho guanine nucleotide exchange factor 39; *Ticam2*—TIR domain-containing adaptor molecule 2; *Rtkn2*—rhotekin 2; *Rad51*—RAD51 recombinase; *Angptl2*—angiopoietin-like 2; *Cxcr4*—C-X-C motif chemokine receptor 4; *Esco2*—establishment of sister chromatid cohesion N-acetyltransferase 2; *Ncapd2*—non-SMC condensin I complex subunit D2; *Arhgap11a*—Rho GTPase-activating protein 11A; *Smc2*—structural maintenance of chromosomes 2; *Ccnd2*—cyclin D2; *Slc43a1*—solute carrier family 43 member 1; *Mad2l1*—mitotic arrest deficient 2-like 1; *Crybg3*—crystallin beta-gamma domain containing 3; *Dcc*—DCC netrin 1 receptor; *Cdc25b*—cell division cycle 25B. F. KEGG pathway enrichment of the target genes.

**图5　正常发育小脑中差异表达miRNAs/mRNAs的Hh通路依赖性、与SHH-MB模型的比较及靶基因KEGG通路富集分析**

**Fig 5**　Hh pathway dependence of differentially expressed miRNAs/mRNAs in the developing cerebellum, comparison with SHH-MB models, and KEGG pathway enrichment of target genes

期、人乳头瘤病毒（human papillomavirus，HPV）感染、细胞衰老等过程（图6G）。

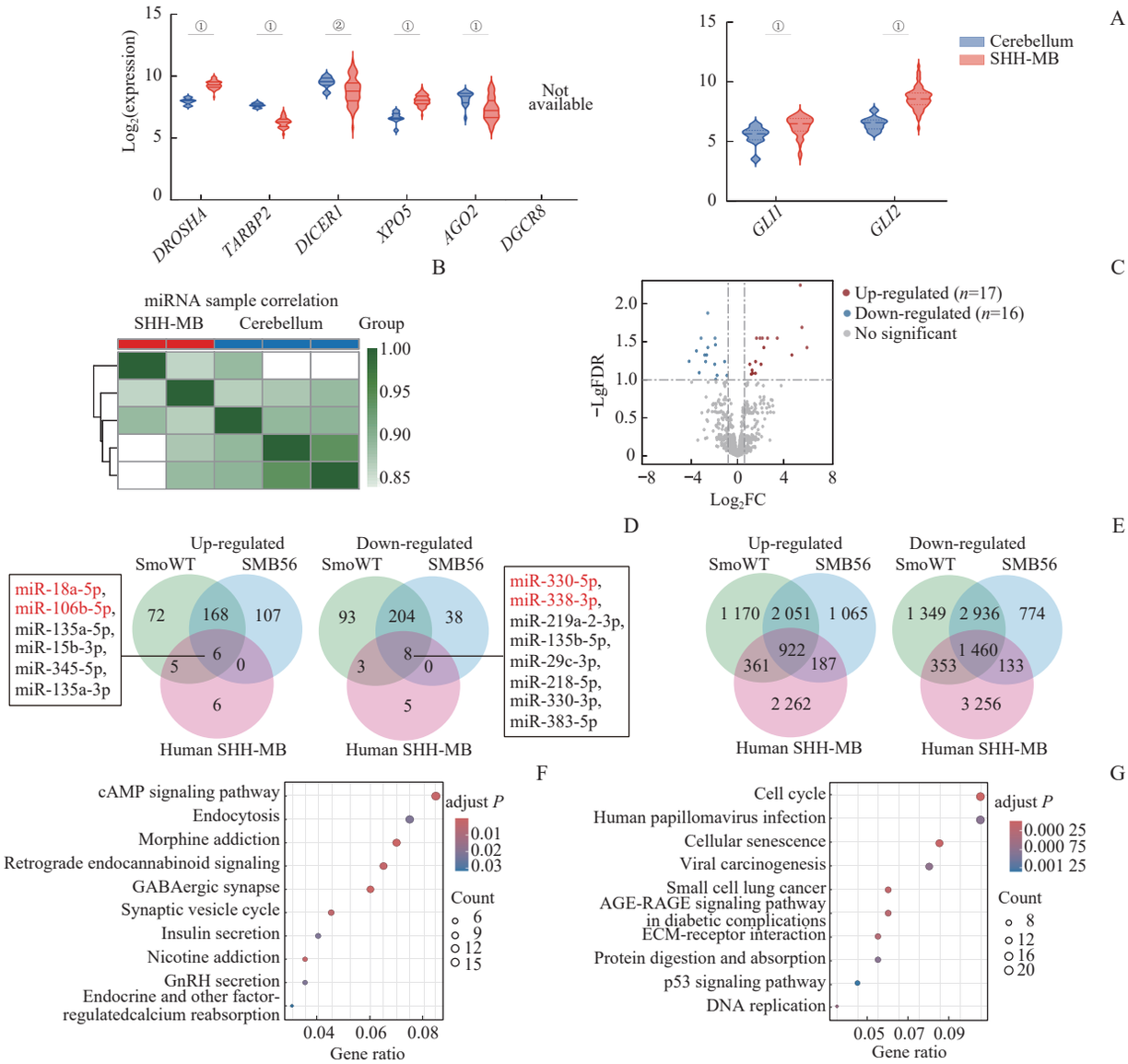


**Note**：A. mRNA expression of Hh pathway genes (*GLI1*, *GLI2*) and miRNA biogenesis genes in SHH-MB patient tumors and normal cerebellum tissues (U133p2 dataset; ①$P$<0.001, ②$P$=0.010). B. Correlation analysis of miRNA expression profiles in SHH-MB patient tumors and normal cerebellum tissues (GSE42657 dataset). C. Volcano plot of differentially expressed miRNAs between SHH-MB and normal cerebellum tissues (GSE42657 dataset). FDR—false discovery rate; FC—fold change. D. Conserved differentially expressed miRNAs between SHH-MB patient tumors and mouse SHH-MB models. E. Conserved differentially expressed mRNAs between SHH-MB patient tumors and mouse SHH-MB models. F/G. KEGG pathway enrichment of predicted target genes of conserved up-regulated miRNAs (F) and down-regulated miRNAs (G). AGE—advanced glycation end products; RAGE—receptor for advanced glycation end products; ECM—extracellular matrix.

**图6 SHH-MB患者肿瘤组织miRNAs/mRNAs表达特征及人鼠保守性分析**

**Fig 6** Expression characteristics of miRNAs/mRNAs in tumor tissues from SHH-MB patients and human-mouse conservation analysis

## 3 讨论

目前，领域所熟知的SHH-MB具有显著的致癌Hh通路激活的转录组特征是基于mRNA水平来定义的，而对于miRNA是否可作为Hh通路下游效应靶基因在SHH-MB发生中发挥作用尚缺乏系统的研究。本研究分析了已发表的2个鼠源SHH-MB模型的CRISPR-Cas9筛选结果后发现，miRNA合成与功能相关基因中的*Drosha*和*Dgcr8*不论在肿瘤的体外还是体内生长均表现出显著的依赖性，表明miRNA在鼠源SHH-MB中发挥了重要作用。然而，鉴于miRNA合成与功能相关基因的转录水平在鼠源SHH-MB模型中并未与正常小脑对照之间表现出显著差异，我们认为鼠源SHH-MB中miRNA的表达或功能并没有发生整体性失调。因此，

进一步通过系统检测2个鼠源SHH-MB模型与正常小脑对照中的miRNA表达谱来鉴定鼠源SHH-MB模型中的表达失调miRNA。miRNA表达谱相关性分析的结果显示2个SHH-MB模型具有高度相似的整体miRNA表达谱特征，且都与正常小脑对照存在显著差异。2个模型中一致性显著上调的miRNA包含多个miR17/92家族成员（如miR-17-5p、miR-19a-3p、miR-20a-5p、miR-19b-1-5p），该家族被报道在SHH-MB中高表达且有助于小鼠小脑的发育和GNPs的增殖[34-35]；一致性显著下调的miRNA包含miR-218-5p，既往研究发现其表达下调能够引起表皮生长因子受体（epidermal growth factor receptor，Egfr）、B细胞淋巴瘤2（B-cell lymphoma 2，Bcl-2）等靶标mRNA的表达上调，从而促进肿瘤侵袭和转移[43-45]。同时，本研究对上述miRNA开展疾病相关富集分析也发现，MB是富集的前十名疾病中唯一的肿瘤类型。以上结果均提示，本研究的鼠源SHH-MB模型的miRNA表达谱数据是可靠的。通过对P7正常小脑相较于P60正常小脑的mRNA差异表达结果进行比较后发现，鼠源SHH-MB模型中mRNA表达失调有部分是通过放大P7小脑组织的部分mRNA特征而获得的，进一步印证了鼠源SHH-MB的发育起源是来自生理性Hh通路激活的GNPs。

本研究通过分析GDC-0449处理对鼠源SHH-MB模型以及裸鼠P7小脑的miRNA表达谱的影响，评估Hh通路在发育与肿瘤背景下的调控作用。结果显示，Hh通路对2个SHH-MB模型的miRNA表达调控程度有限，对P7小脑的调控作用更弱，且三者之间由Hh通路驱动的差异表达miRNA重叠度极低，这些模型间异质性是否与*Trp53*遗传背景相关仍有待后续验证。然而Hh通路依赖miRNA，其下游靶基因却共同富集于多个已知的SHH-MB相关致癌通路，提示其可能通过相似机制促进肿瘤的发生，即实现“殊途同归”。而与上述发现形成对比的是，2个SHH-MB模型中非Hh通路依赖的miRNA表达谱具有较高重叠度。由于本研究聚焦于Hh通路依赖的miRNA致癌分子机制，对于肿瘤模型与P7小脑之间非Hh通路依赖失调miRNA之间的相似性分析，以及这些非Hh通路依赖失调miRNA的潜在上游转录调控机制与下游靶基因功能均留待后续研究。

与此同时，本研究还关注了人鼠SHH-MB之间保守的miRNAs/mRNAs调控对。基于临床样本数据，我们发现患者肿瘤中鉴定的差异表达miRNA和mRNA均与2个鼠源SHH-MB模型具有较高重叠度。在此基础上，本课题组后续将扩大SHH-MB患者组织及类器官模型的miRNA表达谱检测规模，以系统构建人源SHH-MB的miRNA失调图谱。针对人鼠共有的保守miRNA，我们也将深入解析其上游转录调控及下游促癌机制，并在人鼠模型中评估其作为治疗靶点的潜力，旨在为SHH-MB的精准治疗提供新靶点与相关策略。

**利益冲突声明/Conflict of Interests**

所有作者声明不存在利益冲突。

All authors disclose no relevant conflict of interests.

**伦理批准和动物权利声明/Ethics Approval and Animal Right**

本研究涉及的所有动物实验均已通过上海交通大学基础医学院科研伦理委员会的审核批准[批准号：A2022-033]。所有实验过程均参照《实验动物管理条例》的规定执行。

All experimental animal protocols in this study were reviewed and approved by the Scientific Research Ethics Committee of Shanghai Jiao Tong University College of Basic Medical Sciences [Approval Letter No. A2022-033], and all experimental animal protocols were carried out by following the guidelines of *Regulations for the Administration of Affairs Concerning Experimental Animals*.

**作者贡献/Authors′Contributions**

朱颖参与实验设计、实验实施、数据分析、论文写作与修改，隋怡参与前期实验设计与实施、论文的写作及修改，唐玉杰全程指导课题开展、论文写作与修改。所有作者均阅读并同意了最终稿件的提交。

Zhu Ying participated in experiment design, experiment implementation, data analysis, and paper writing and modification. Sui Yi participated in the preliminary experimental design and implementation, as well as paper writing and revision. Tang Yujie supervised the whole project development, and paper writing and revision. All authors have read the last version of paper and consented to submission.

· Received: 2025-07-02
· Accepted: 2025-11-25
· Published online: 2026-01-12

## 参·考·文·献

[1] Ostrom Q T, Price M, Neff C, et al. CBTRUS statistical report: primary brain and other central nervous system tumors diagnosed in the United States in 2016-2020[J]. Neuro Oncol, 2023, 25(12 Suppl 2): iv1-iv99.

[2] Hovestadt V, Ayrault O, Swartling F J, et al. Medulloblastomics

revisited: biological and clinical insights from thousands of patients[J]. Nat Rev Cancer, 2020, 20(1): 42-56.
[3] Kool M, Korshunov A, Remke M, et al. Molecular subgroups of medulloblastoma: an international meta-analysis of transcriptome, genetic aberrations, and clinical data of WNT, SHH, Group 3, and Group 4 medulloblastomas[J]. Acta Neuropathol, 2012, 123(4): 473-484.
[4] Northcott P A, Shih D J H, Peacock J, et al. Subgroup-specific structural variation across 1, 000 medulloblastoma genomes[J]. Nature, 2012, 488(7409): 49-56.
[5] Northcott P A, Robinson G W, Kratz C P, et al. Medulloblastoma[J]. Nat Rev Dis Primers, 2019, 5(1): 11.
[6] Thayer S P, Di Magliano M P, Heiser P W, et al. Hedgehog is an early and late mediator of pancreatic cancer tumorigenesis[J]. Nature, 2003, 425(6960): 851-856.
[7] Mao J H, Ligon K L, Rakhlin E Y, et al. A novel somatic mouse model to survey tumorigenic potential applied to the Hedgehog pathway[J]. Cancer Res, 2006, 66(20): 10171-10178.
[8] Pugh T J, Weeraratne S D, Archer T C, et al. Medulloblastoma exome sequencing uncovers subtype-specific somatic mutations[J]. Nature, 2012, 488(7409): 106-110.
[9] Kieran M W, Chisholm J, Casanova M, et al. Phase I study of oral sonidegib (LDE225) in pediatric brain and solid tumors and a phase II study in children and adults with relapsed medulloblastoma[J]. Neuro Oncol, 2017, 19(11): 1542-1552.
[10] Lorusso P M, Rudin C M, Reddy J C, et al. Phase I trial of hedgehog pathway inhibitor vismodegib (GDC-0449) in patients with refractory, locally advanced or metastatic solid tumors[J]. Clin Cancer Res, 2011, 17(8): 2502-2511.
[11] Atwood S X, Li M, Lee A, et al. GLI activation by atypical protein kinase C ι/λ regulates the growth of basal cell carcinomas[J]. Nature, 2013, 494(7438): 484-488.
[12] Buonamici S, Williams J, Morrissey M, et al. Interfering with resistance to smoothened antagonists by inhibition of the PI3K pathway in medulloblastoma[J]. Sci Transl Med, 2010, 2(51): 51ra70.
[13] Kool M, Jones D T W, JäGer N, et al. Genome sequencing of SHH medulloblastoma predicts genotype-related response to smoothened inhibition[J]. Cancer Cell, 2014, 25(3): 393-405.
[14] Rack P G, Ni J, Payumo A Y, et al. Arhgap36-dependent activation of Gli transcription factors[J]. Proc Natl Acad Sci USA, 2014, 111(30): 11061-11066.
[15] Zhao X S, Ponomaryov T, Ornell K J, et al. RAS/MAPK activation drives resistance to SMO inhibition, metastasis, and tumor evolution in SHH pathway-dependent tumors[J]. Cancer Res, 2015, 75(17): 3623-3635.
[16] Hogg S J, Beavis P A, Dawson M A, et al. Targeting the epigenetic regulation of antitumour immunity[J]. Nat Rev Drug Discov, 2020, 19(11): 776-800.
[17] Zhang B H, Pan X P, Cobb G P, et al. microRNAs as oncogenes and tumor suppressors[J]. Dev Biol, 2007, 302(1): 1-12.
[18] Liu F, Jiang W Y, Sui Y, et al. CDK7 inhibition suppresses aberrant hedgehog pathway and overcomes resistance to smoothened antagonists[J]. Proc Natl Acad Sci USA, 2019, 116(26): 12986-12995.
[19] Pak E, Mackenzie E L, Zhao X S, et al. A large-scale drug screen identifies selective inhibitors of class I HDACs as a potential therapeutic option for SHH medulloblastoma[J]. Neuro Oncol, 2019, 21(9): 1150-1163.
[20] Mo J L, Liu F, Sun X, et al. Inhibition of the FACT complex targets aberrant hedgehog signaling and overcomes resistance to smoothened antagonists[J]. Cancer Res, 2021, 81(11): 3105-3120.
[21] Tang Y J, Gholamin S, Schubert S, et al. Epigenetic targeting of Hedgehog pathway transcriptional output through BET bromodomain inhibition[J]. Nat Med, 2014, 20(7): 732-740.
[22] Murchison E P, Hannon G J. miRNAs on the move: miRNA biogenesis and the RNAi machinery[J]. Curr Opin Cell Biol, 2004, 16(3): 223-229.
[23] Siomi H, Siomi M C. Posttranscriptional regulation of microRNA biogenesis in animals[J]. Mol Cell, 2010, 38(3): 323-332.
[24] Lin S B, Gregory R I. MicroRNA biogenesis pathways in cancer[J]. Nat Rev Cancer, 2015, 15(6): 321-333.
[25] Pereira D M, Rodrigues P M, Borralho P M, et al. Delivering the promise of miRNA cancer therapeutics[J]. Drug Discov Today, 2013, 18(5/6): 282-289.
[26] Mitchell P S, Parkin R K, Kroh E M, et al. Circulating microRNAs as stable blood-based markers for cancer detection[J]. Proc Natl Acad Sci USA, 2008, 105(30): 10513-10518.
[27] Abu-Halima M, Keller A, Becker L S, et al. Dynamic and static circulating cancer microRNA biomarkers: a validation study[J]. RNA Biol, 2023, 20(1): 1-9.
[28] Kalhori M R, Soleimani M, Arefian E, et al. The potential role of miR-1290 in cancer progression, diagnosis, prognosis, and treatment: an oncomiR or onco-suppressor microRNA? [J]. J Cell Biochem, 2022, 123(3): 506-531.
[29] Tanigawa K, Misono S, Mizuno K, et al. MicroRNA signature of small-cell lung cancer after treatment failure: impact on oncogenic targets by miR-30a-3p control[J]. Mol Oncol, 2023, 17(2): 328-343.
[30] Hong D, Zang A M, Wang Z Y, et al. Elevation of microRNA-365 impedes malignant behaviors of gastric cancer cells by inhibiting PAX6[J]. Funct Integr Genomics, 2022, 22(5): 825-834.
[31] Salm F, Dimitrova V, Von Bueren A O, et al. The phosphoinositide 3-Kinase p110α isoform regulates leukemia inhibitory factor receptor expression *via* c-Myc and miR-125b to promote cell proliferation in medulloblastoma[J]. PLoS One, 2015, 10(4): e0123958.
[32] Lv S Q, Kim Y H, Giulio F, et al. Genetic alterations in microRNAs in medulloblastomas[J]. Brain Pathol, 2012, 22(2): 230-239.
[33] Jiang Z H, Cushing L, Ai X B, et al. miR-326 is downstream of Sonic hedgehog signaling and regulates the expression of Gli2 and smoothened[J]. Am J Respir Cell Mol Biol, 2014, 51(2): 273-283.
[34] Northcott P A, Fernandez-L A, Hagan J P, et al. The miR-17/92 polycistron is up-regulated in sonic hedgehog-driven medulloblastomas and induced by N-myc in sonic hedgehog-treated cerebellar neural precursors[J]. Cancer Res, 2009, 69(8): 3249-3255.
[35] Murphy B L, Obad S, Bihannic L, et al. Silencing of the miR-17~92 cluster family inhibits medulloblastoma progression[J]. Cancer Res, 2013, 73(23): 7068-7078.
[36] Sui Y, Wang T, Mei Y Q, et al. Targeting super-enhancer-driven transcriptional dependencies suppresses aberrant hedgehog pathway activation and overcomes smoothened inhibitor resistance[J]. Cancer Res, 2024, 84(16): 2690-2706.
[37] Kozomara A, Birgaoanu M, Griffiths-Jones S. miRBase: from microRNA sequences to function[J]. Nucleic Acids Res, 2019, 47(D1): D155-D162.
[38] Jones T A, Jeyapalan J N, Forshew T, et al. Molecular analysis of pediatric brain tumors identifies microRNAs in pilocytic astrocytomas that target the MAPK and NF-κB pathways[J]. Acta Neuropathol Commun, 2015, 3: 86.
[39] Laresgoiti U, Apraiz A, Olea M, et al. E2F2 and CREB cooperatively regulate transcriptional activity of cell cycle genes[J]. Nucleic Acids Res, 2013, 41(22): 10185-10198.
[40] Xia Y H, Zhen L, Li H X, et al. MIRLET7BHG promotes hepatocellular carcinoma progression by activating hepatic stellate cells through exosomal SMO to trigger Hedgehog pathway[J]. Cell Death Dis, 2021, 12(4): 326.
[41] Zhang P X, Gao H, Yan R P, et al. has_circ_0070512 promotes prostate cancer progression by regulating the miR-338-3p/hedgehog signaling pathway[J]. Cancer Sci, 2023, 114(4): 1491-1506.
[42] Tschaikner P, Enzler F, Torres-Quesada O, et al. Hedgehog and Gpr161: regulating cAMP signaling in the primary Cilium[J]. Cells, 2020, 9(1): 118.
[43] Venkataraman S, Birks D K, Balakrishnan I, et al. microRNA 218 acts as a tumor suppressor by targeting multiple cancer phenotype-associated genes in medulloblastoma[J]. J Biol Chem, 2013, 288(3): 1918-1928.
[44] Zhu K G, Ding H Y, Wang W G, et al. Tumor-suppressive miR-218-5p inhibits cancer cell proliferation and migration *via* EGFR in non-small cell lung cancer[J]. Oncotarget, 2016, 7(19): 28075-28085.
[45] Mollashahi B, Aghamaleki F S, Movafagh A. The roles of miRNAs in medulloblastoma: a systematic review[J]. J Cancer Prev, 2019, 24(2): 79-90.

［本文编辑］ 邢宇洋